

Design of a Process for Supercritical Water Desalination with Zero Liquid Discharge

Samuel O. Odu,[†] Aloïsius G. J. van der Ham,^{*,†} Sybrand Metz,[‡] and Sascha R. A. Kersten[†]

[†]Sustainable Process Technology, Faculty of Science and Technology, University of Twente, Drienerlolaan 5, 7522 NB Enschede, The Netherlands

[‡]Wetsus, European Center of Excellence for Sustainable Water Technology, Oostergoweg, 98911 MA Leeuwarden, The Netherlands

ABSTRACT: Conventional desalination methods have a major drawback; the production of a liquid waste stream which must be disposed. The treatment of this waste stream has always presented technical, economic, and environmental challenges. The supercritical water desalination (SCWD) process meets these challenges as it allows for the treatment of salt-water streams with zero liquid discharge (ZLD). An experimental apparatus has been designed, built, and operated to show the proof of principle of the SCWD process using NaCl–H₂O as a model solution. Next, a SCWD process with a two-stage separation step was designed. Enthalpy calculations for a 3.5 wt % NaCl feed and experimental results show that the SCWD process operated at 460 °C and 300 bar will produce drinking water (750 ppm total dissolved solids) and salt crystals (2–5 μm) with an estimated stand-alone thermal energy consumption of 450 MJ_{th}/m³ product water.

1. INTRODUCTION

Desalination, the process of removing salt from salt water streams to produce fresh water remains a viable means to abate the global challenge of water scarcity.¹ The continual research and development of desalination processes over the decades have resulted in a variety of commercial desalination methods. These processes can be classified into major desalting processes such as multistage flash distillation (MSF), multiple effect distillation (MED), vapor compression (VC) and reverse osmosis (RO), and minor desalting processes such as freezing, solar humidification, and electro dialysis, with respect to their installed capacities and commercial successes.² MSF and RO are the most widely used desalination methods to obtain fresh water from salt-water (seawater and brackish water) streams.

MSF units are widely used in the Middle East (particularly in Saudi-Arabia, the United Arab Emirates, and Kuwait) and they account for over 40% of the world's desalination capacity.³ Although this desalination method produces water of very good quality (approximately 50 ppm of TDS), it has two major drawbacks: (i) low fresh water to feed ratio (about 50% for seawater installations) and, (ii) the production of a waste brine stream (70 000 ppm TDS for seawater installations) which needs to be handled somehow.

Reverse osmosis (RO) is a very appealing process for saline water desalination, and is becoming a leading method in the commercial desalination industry.² An important factor that has influenced the advances of the reverse osmosis process is its lower energy consumption (30 MJ_{el}/m³ drinking water³) compared to MSF plants (300 MJ_{th}/m³ drinking water^{3–6}). Feed concentration affects the performance of RO plants. For example, while a yield (defined as ratio of fresh water produced to feedwater) of 90–95% can be obtained for brackish water installations, only a value of 35–50% is achieved for seawater processing due to the high osmotic pressure.⁷ Drawbacks of the RO process include membrane fouling,⁸ and the production of

a waste brine stream (~60 000 ppm for seawater installations) which contains antiscalining agents and antiflocculants.

The brine streams from MSF and RO processes are usually discharged in the ocean if the desalination plant is located close to the coast, otherwise, an extra treatment step is required if the plant is located inland. Discarding the concentrated brine in the ocean leads to local increased salinity and turbidity which could lead to negative impact on marine ecology.⁹ With the expected more stringent regulations regarding dilution in surface water,¹⁰ a new desalination method which avoids the production of concentrated brine stream needs to be investigated. In this paper, we present a process called supercritical water desalination (SCWD). This process allows for the treatment of salt-water streams without the production of an aqueous waste stream (zero liquid discharge concept), and offers an increased water yield (>93% for a seawater installation).

Supercritical water (SCW) is defined as water at pressures and temperatures above the critical pressure ($P_c = 221.2$ bar) and critical temperature ($T_c = 374.15$ °C) of water. As water approaches the supercritical state, its properties change drastically. Such changes in properties include lower density, decreased viscosity, lower dielectric constant and diminished hydrogen bonding compared to water at ambient conditions.^{11,12} The changes in hydrogen bonding and dielectric constant make water lose its polarity and consequently its solvation ability for inorganic compounds/salts. The solubility of inorganic salts in water drops by several orders of magnitude when water enters the supercritical (SC) state. As a result inorganic salts precipitate to form solid salts within the supercritical water system.^{13–15} The diminished solubility of

Received: March 2, 2015

Revised: April 21, 2015

Accepted: April 22, 2015

Published: April 22, 2015

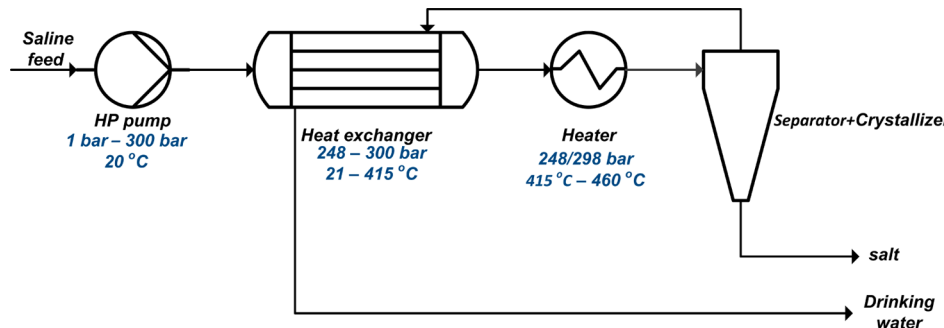


Figure 1. Conceptual design of the SCWD process.

inorganic salts in supercritical water is the principle employed in the SCWD process.

A conceptual design for the SCWD process is shown in Figure 1. A high-pressure pump is required to pressurize the saline feed to pressures above the critical pressure of water. Because the process is energy intensive (approximately 2 GJ of energy is required to bring 1 m³ of water from room conditions, $P = 1.02$ bar, $T = 25$ °C, to supercritical conditions, $P_c = 221$ bar, $T_c = 375$ °C), a heat exchanger that operates at sub- to supercritical water conditions is necessary to recover most of the energy supplied to the process. A heater that provides additional energy is required to bring the feed to the desired temperature necessary for separation. Key design challenges that have been identified are (i) the controlled removal of salts at these supercritical conditions, (ii) the high level of heat integration in order for the process to be economically viable, and (iii) selection of materials of construction that can withstand the extreme conditions of temperature, pressure, and chemical corrosion. Solutions to these major challenges will be discussed subsequently in this paper.

To design a SCWD unit, it is essential to know the phases that are present at supercritical water conditions and understand the effect of process conditions (pressure and temperature) on separation efficiency. The phases present at supercritical conditions for a saline solution (sodium chloride–water is used as a model system) will be investigated in a small-scale quartz capillary tube. The effects of pressure, temperature, and feed concentration on separation and energy requirements will also be studied. The results of these investigations will form the basis for the selection of a separation unit as well as help to identify the optimal operating conditions for a desired level of separation at minimum energy costs.

2. EXPERIMENTAL SECTION

2.1. Experiments and Procedures. The experiments are divided into two parts: visualization experiments to determine the phases present under supercritical (SC) conditions, and solubility measurements under SC conditions at two pressures (250 and 300 bar) and different temperatures (380–500 °C). The focus is on sodium chloride (NaCl) since it is the main constituent of seawater.

2.1.1. Visualization Experiments. Armellini and co-workers^{16,17} have developed an experimental technique to examine phase behavior and precipitation in salt-water systems near and above the critical point of pure water and study salt nucleation and growth from supercritical water. Their experimental apparatus features an “optically accessible cell” made of Inconel 625 and sapphire windows. This experimental technique offers

the advantage of conducting isobaric experiments; however, it is expensive and could not be readily purchased.

To study the phases present at SC conditions for sodium chloride solution, visualization experiments will be carried out in quartz capillaries. This experimental technique was developed by Potic et al.¹⁸ to study thermochemical conversion of wet biomass at supercritical water conditions. This experimental method has several advantages: (i) an experiment can be conducted that is fast, inexpensive, and safe, (ii) the quartz capillaries can withstand extremely high pressures (600 bar) and high temperatures (900 °C), (iii) quartz capillaries have no catalytic activity, and (iv) quartz is corrosion resistant.¹⁸ A major disadvantage is that isobaric measurements cannot be carried out with this experimental method. Because of the pressure–temperature relationship in isochoric systems, the pressure in the capillary increases as the temperature is increased. However, since water vapor pressure predominantly determines the overall pressure, the pressure in the quartz capillary can be controlled by the initial amount of solution in the capillary.¹⁸ The P – T relationship for water in a closed system¹⁹ is used to estimate the pressures in the capillary at the various recorded temperatures.

In the experiments, a sodium chloride solution (3.5 wt %, about the same amount present in seawater) was injected into a quartz capillary (i.d. = 1 mm; o.d. = 2 mm; length = 170 mm; liquid level = 20 mm). The capillary is then sealed and put into an oven with a sight glass at the front (see Figure 2). A thermocouple (TI-C) is attached to the outer wall of the

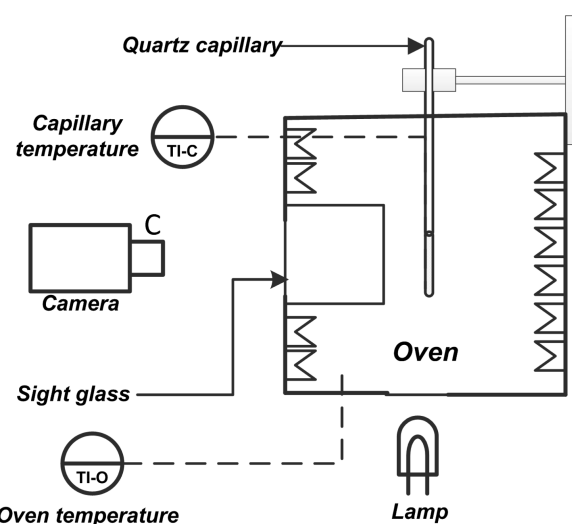


Figure 2. Schematic of apparatus for visualization experiments.

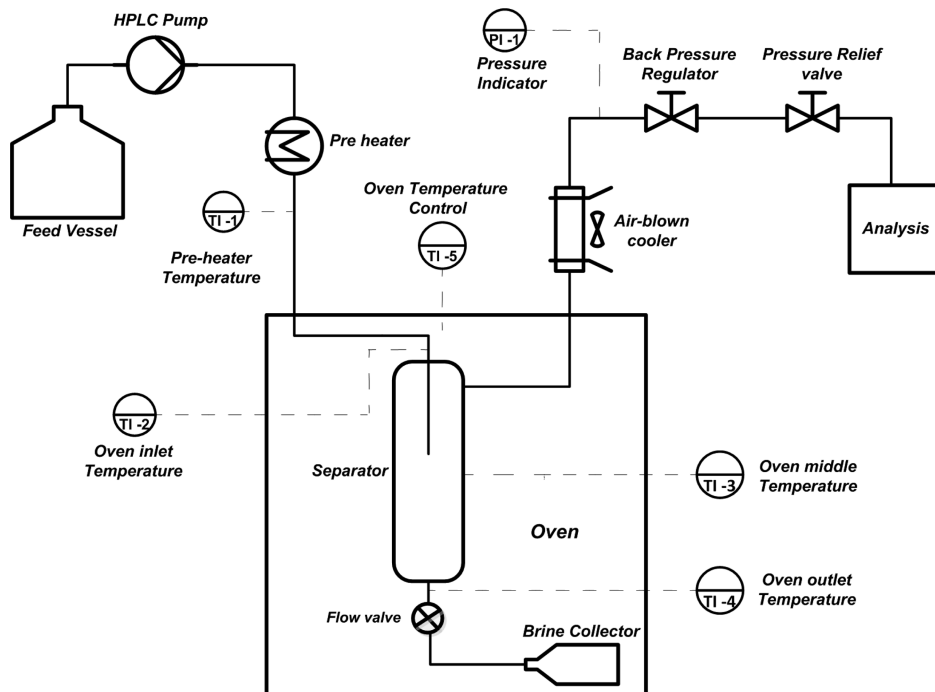


Figure 3. Schematic of experimental set-up for phase equilibrium measurement.

capillary to measure the temperature. This wall temperature is taken as the temperature in the capillary. A video camera is positioned in front of the oven for recording. Because the system is closed (isochoric), the temperature and pressure inside the quartz capillary are interrelated. However, the maximum pressure the system can attain for a desired temperature can be controlled by the amount of liquid that is injected in the quartz capillary. The quartz capillary can be operated up to 300 bar and 500 °C with the initial liquid level used in these visualization experiments.

2.1.2. Phase Equilibrium Measurements. The visualization experiments present some insight into the phases present and phase changes that occur at supercritical conditions for a 3.5 wt % sodium chloride solution. To determine the concentration of the salt in the phases observed in the visualization experiments, solubility measurements at phase equilibrium were carried out.

The equilibrium phase behavior of NaCl–H₂O system under supercritical water conditions was investigated in the past. Olander and Liander,²⁰ Parisod and Plattner,²¹ Bischoff et al.,²² Sourirajan and Kennedy,²³ and Armellini and Tester²⁴ have all investigated the phase behavior of the NaCl–H₂O system under isothermal conditions at supercritical water pressures and temperatures. Bischoff and Pitzer,²⁵ and Armellini²⁶ presented temperature–composition phase diagrams for NaCl–H₂O at 250 and 300 bar respectively by interpolating the isothermal data of several of the authors mentioned above. A recent study by Leusbroek et al.¹³ presents solubility data for sodium chloride in water at temperature and pressure ranges of 380–420 °C and 180–235 bar, respectively.

Although the solubility and equilibrium phase diagram of NaCl have been studied extensively, there are discrepancies (orders of magnitude in some cases) in the data reported in literature by different authors under the same experimental conditions (e.g., see refs 23 and 26). In addition, extrapolating experimental data points beyond the experimental condition range can lead to possible errors. The SCWD process will

operate under isobaric supercritical water conditions, interpolating isothermal data found in literature might lead to possible errors in the solubility of NaCl in the pressure and temperature range of interest to the process; therefore, it is decided to measure the solubility of NaCl in supercritical water at these process conditions in the vapor and liquid phase in one experiment. The apparatus was also used for the proof of concept of the separation method.

To determine the temperature–composition phase diagram of NaCl–H₂O under isobaric conditions, an experimental setup that can be used to measure the solubility of salt in the vapor (supercritical) phase and liquid phase has been designed and built (see Figure 3). The experimental set up is a modification of the one used by Leusbroek et al.¹³ The design of the separator is similar to that used by Vogel et al.²⁷ to study the separation performance of various binary type I salt–water mixtures.

Pressures up to 400 bar were provided to the unit using a HPLC pump (LabAlliance series 1500, LabAlliance USA) with a volume flow rate of 0.01–12 mL/min and controlled with a back pressure regulator (TESCOM 26-1762-24-S, Tescom Europe GmbH & Co. KG, Germany, C_v = 0.1, accuracy ± 1 % of central pressure range). Electrical heating is provided in the preheater and oven. The preheater is used to raise the temperature of the pressurized feed from room temperature to about 250 °C. Owing to the very corrosive nature of chloride containing feeds at subcritical temperatures,²⁸ titanium grade 1 (Ethen Rohre GmbH, Germany) is used for the tubing between the preheater and the oven. Inside the oven, a cylindrical vessel (separator) is installed, in which the phase separation occurs. The separator is made of Incoloy 825 with an internal diameter of 10 mm and a length of 85 mm. Standard type K thermocouples (accuracy ±0.75%) are installed in the preheater and oven to measure and control the temperatures therein. Thermocouples are also attached to the inlet (TI-2), middle (TI-3) and outlet (TI-4) of the separator to measure the

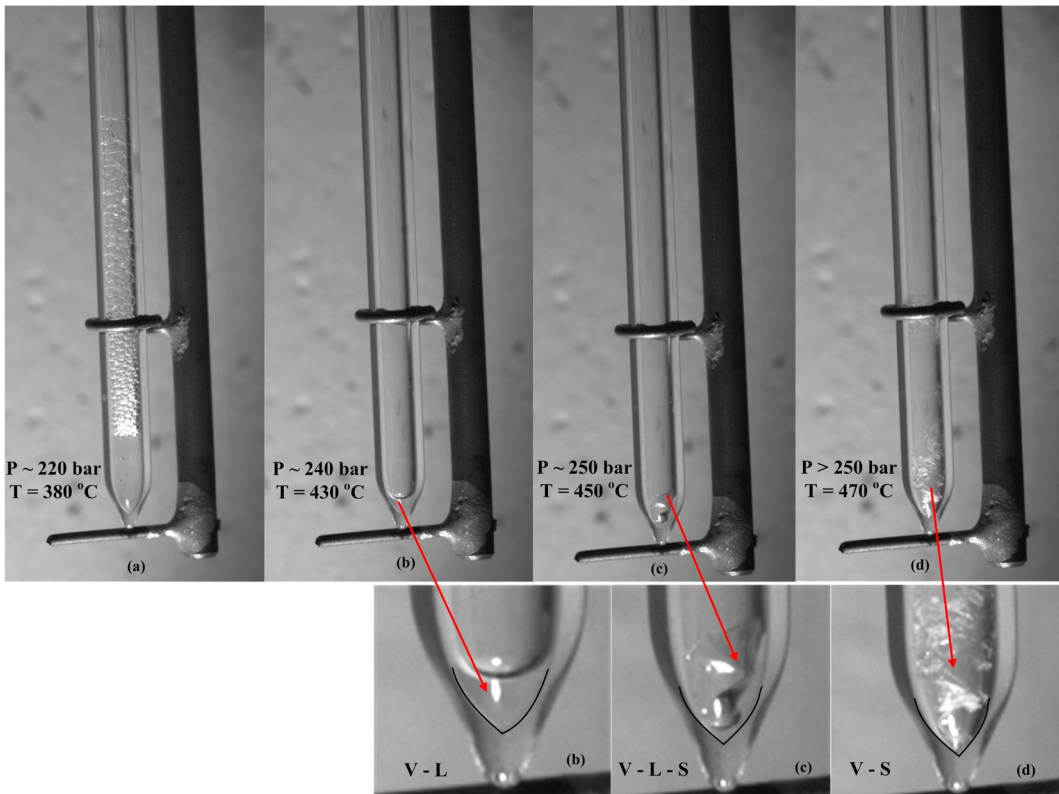


Figure 4. Photographs showing the phases present at different temperatures in SCW for 3.5 wt % NaCl solution at start. In the enlargements the interface between the glass and liquid phase has been accentuated with a solid line.

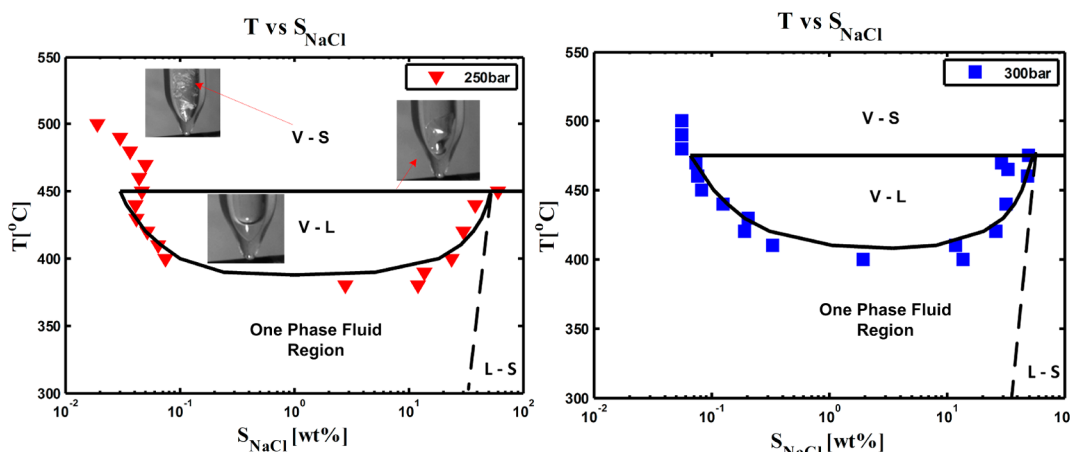


Figure 5. Phase diagrams of NaCl at 250 bar (with photos of capillary experiment) and 300 bar, and supercritical temperatures: — compilation of Bischoff and Pitzer;²⁵ ---, estimated from Linke.³⁰

temperatures at these points, and the average of the three temperatures is taken as the temperature in the separator. The mean absolute deviation of the temperatures recorded by the three thermocouples (TI-2, TI-3, and TI-4) is 2 °C.

The saline feed (3.5 wt % NaCl) is prepared using demineralized water and pure sodium chloride (>99.5% purity) from Sigma-Aldrich (Sigma-Aldrich Chemie, GmbH, Germany). The temperatures in the preheater and oven as well as the pressure are then set to the desired values. Saline feed is supplied to the unit at a flow rate of 0.2 mL/min. The feed is preheated to a temperature of 250 °C, and further heating to the desired temperature is achieved in the oven via electrical heating. Inside the separator in the oven, phase separation takes

place with the supercritical phase (product water stream) leaving from the top while the liquid (brine) phase stays in the separator. The outgoing supercritical phase is cooled (with a fan), depressurized to room conditions, and collected for analysis. This is done at an interval of 20 min. The system is deemed to be in equilibrium when deviations in three consecutive solubility measurements are ± 0.001 wt % (10 ppm).

When equilibrium is ascertained, the resulting liquid phase (brine) is collected under experimental conditions (pressure and temperature), into a liquid collector (0.5 mL) with the aid of an air-controlled flow valve (see Figure 3). The salt concentration of the product water stream and the brine

collected (after dilution with a known amount of demineralized water) are determined via conductivity measurement. Mass in and out of the experimental setup were measured to ascertain if the mass balance is closed. The mass balance error was calculated to be less than 2% (relative standard error) on a salt basis.

3. RESULTS: VISUALIZATION AND PHASE EQUILIBRIUM MEASUREMENTS

As the solution in the quartz capillary is heated (Figure 2), the pressure in the system increases with increasing temperature (the system is isochoric). Photographs taken during the visualization experiments are shown in Figure 4. At temperatures and pressures above the critical point of pure water ($T_c = 374^\circ\text{C}$, $P_c = 221$ bar), two distinct regions exist. At 380°C (pressure equivalent of about 220 bar), the first bubbles appeared (Figure 4a) resulting in the formation of a vapor–liquid (V–L) region in the system. With continued heating, the existence of a V–L phase was observed, and as the temperature increases, the liquid level in the capillary decreases (Figure 4b), resulting in an increase in salt concentration in the liquid phase. At 450°C (approximately 250 bar), a transition vapor–liquid–solid (V–L–S) region appears (Figure 4c), and the system enters a vapor–solid (V–S) region (Figure 4d). These observations are consistent with the behavior of a Type I salt–water system.²⁶

To check the effect of the feed concentration on separation, the experiment was repeated with sodium chloride solutions with initial concentrations of 1, 5, and 10 wt %. The temperatures at which the phase transitions occurred remain unchanged, which suggests that the initial feed concentration has no effect on the degree of separation. However, the volume of liquid observed in the V–L region increases with an increase in initial concentration.

The observations made in the visualization experiments are more evident in the solubility measurements as presented in Figure 5. This figure shows the results of solubility measurements for sodium chloride in the vapor phase and liquid phase at pressures of 250 and 300 bar and supercritical temperatures (380 – 500°C). An important feature of the phase diagrams at these two pressures is the existence of a vapor–liquid phase region at temperatures above the supercritical temperature of pure water ($T_c = 374^\circ\text{C}$). The measurements presented in this study are in agreement with the temperature–composition compilation of Bischoff and Pitzer,²⁵ and the phase diagram of Armellini²⁶ obtained by interpolating isothermal data of several authors (see section 2.1.2, Phase Equilibrium Measurements). The solubility results also show that drinking water within the set safe limit (1000 ppm TDS²⁹) can be produced within the V–L region. For example, at 300 bar and 460°C , the quality of water produced is 750 ppm (see Figure 5). Thus, by controlling the temperature in the separator (Figure 3), solids formation, which can lead to equipment blockage, can be avoided.

This principle will be applied in the final design by having a two-stage separation. First, a V–L separator to remove the supercritical product water from the liquid phase at 250/300 bar followed by a V–S separator to obtain the solid salt by flashing the liquid phase (a highly concentrated salt solution, 50 wt % at 300 bar, 460°C) to atmospheric pressure. The flashing experiment is discussed in the subsequent subsection.

During the phase equilibrium measurements, higher pressure and temperature fluctuations were observed at 250 bar (P fluctuation = ± 5 bar, T fluctuation = $\pm 3^\circ\text{C}$) compared to 300

bar (P fluctuation = ± 1 bar, T fluctuation = $\pm 1^\circ\text{C}$). The phase diagram shifts upward as the pressure is increased from 250 to 300 bar. The quality (measured as TDS) of the water produced also decreased with increased pressure at the same system operating temperature (for example, at 440°C , the concentration of NaCl at 250 bar is 400 ppm, while at 300 bar the concentration is 1000 ppm). These results reveal that a lower pressure of 250 bar favors better quality of produced water; however, an operating pressure of 300 bar favors system stability (low/no fluctuations in pressure and temperature).

The effect of feed concentration on the solubility of NaCl in supercritical water was also investigated for solutions with initial concentrations of 1 and 10 wt %, respectively. The experiments were conducted at pressures of 250 and 300 bar, and temperatures of 380, 420, 450, and 500°C . No noticeable difference in solubility was observed when compared to the 3.5 wt % solution experiments.

3.1. Flash Crystallization of 50 wt % Brine Solution. A slight modification of the experimental setup for phase equilibrium measurements (see Figure 3) has been carried out to enable us to simulate the crystallization of salt when the liquid phase (50 wt % at 300 bar and 460°C) in the V–L region of the phase diagram is flashed to atmospheric pressure. In the modified setup, the brine collector in Figure 3 was replaced with a nozzle (ID = 1.5 mm, length = 160 mm) made from Incoloy 825. The experimental procedure is as described in section 2.1.2, Phase Equilibrium Measurements. The experiment was carried out at 300 bar, 460°C and was also used for the proof of principle of this separation technique.

After phase equilibrium is ascertained, the pump is switched off for about 2–5 min to allow most of the vapor left in the separator to exit the system, the temperature and pressure of the system being monitored the entire time. Afterward, the air-controlled valve is opened, and the liquid phase that was collected in the separator under process conditions is flashed to atmospheric pressure.

The SEM (Jeol JSM 5600 LV, at 5 kV) photomicrograph of the NaCl salt which was used to prepare the feed solution as well as that of the solids obtained after the flash experiment is shown in Figure 6. The feed particles shown in Figure 6a are crystalline with sizes ranging from 200–700 μm . The salt obtained from flashing the 50 wt % brine from 300 bar, 460°C to atmospheric pressure, shown in Figure 6b comprises small particles (size range, 2 to 5 μm) clustered together. At higher magnification, no pores were revealed on the surface of the particles, indicating a crystalline structure. Particle sizes of the crystals will guide the choice and design of the cyclone to separate the salt from the steam.

4. PROCESS SIMULATION

Preliminary process simulations with water in the commercial process simulator UniSim Design Suite were carried out at the two pressures, 250 and 300 bar, to determine how the system operating pressure influences the heat exchanger efficiency and heater duty (Figure 1) required for separation. The temperatures for simulations at the two different pressures have been chosen to avoid solids formation in the real separator. The phase equilibrium measurements, Figure 5, guide the choice of temperature. As such, 440°C is chosen as the operating temperature (for phase separation) at 250 bar, while 460°C is chosen as the system temperature at 300 bar.

The simulation process flow diagram (PFD) of the conceptual design (Figure 1) with the stream table at 300 bar

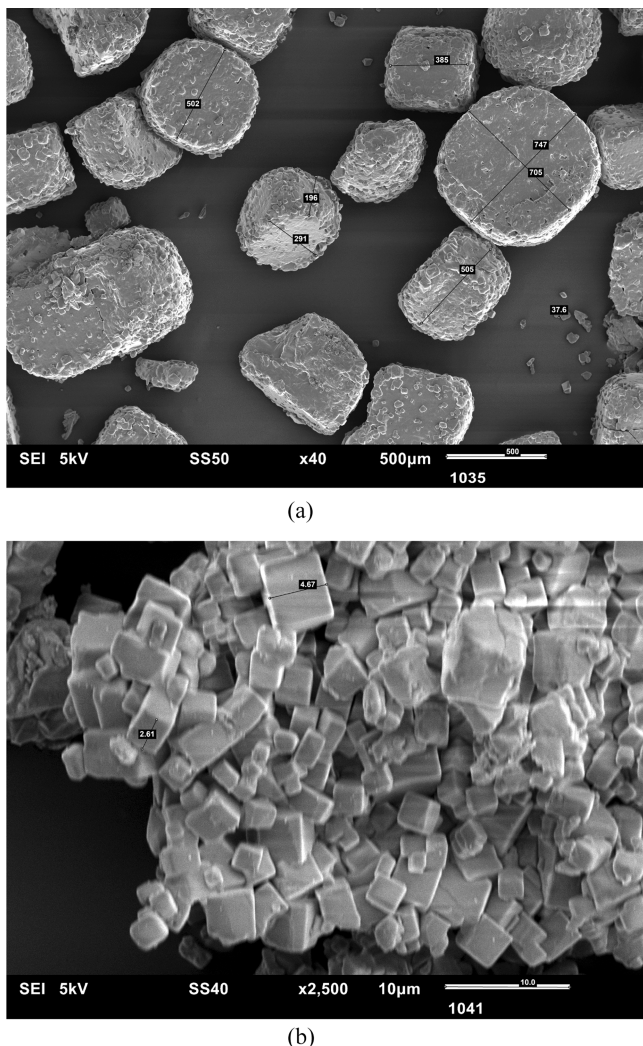


Figure 6. SEM photomicrographs of particles of (a) NaCl feed, (b) NaCl obtained from flashing the brine solution.

is shown in Figure 7. The feed is pressurized and enters a counter-current shell and tube heat exchanger (E-100) where it is preheated with the supercritical water coming from the separator (E-101). The stream then enters the separator (E-

101) where additional heating required for the separation is added. The outlet stream (#3) is split (TEE-101) into 93% (mass basis) supercritical product water (#4) and 7% concentrated liquid (#5), mimicking the V-L separation. Stream #4 is cooled by using it to preheat the feed. Further cooling and depressurization are done in the cooler (E-102) and relief valve (RV-100), respectively.

The performance of the heat exchanger (E-100) and the duty of the heater (E-101) are of interest. To make a fair comparison between the two pressures, the duty, logarithmic temperature difference (LMTD), and overall heat transfer coefficient (U) of the heat exchanger (E-100) are set to the same value (see Table 1) for the two simulations. The minimum approach temper-

Table 1. UniSim Design Simulation Output

	250	300	300 ^a
E-100 duty (GJ _{th} /m ³ product water)	2.5	2.5	2.5
E-100 ΔT_{\min} (°C)	<u>15</u>	<u>20</u>	<u>15</u>
E-100 LMTD (°C)	46	46	33
U (W/m ² ·°C)	1000	1000	1000
A (m ²)	0.15	0.15	0.21
$T_{\#3}$ (°C)	440	460	460
E-101 duty (MJ _{th} /m ³ product water)	<u>670</u>	<u>520</u>	<u>410</u>
P-100 power (MJ _{el} /m ³ product water)	40	50	50

^aSimulation results for a pilot unit (5. Design of a Pilot Unit).

ature (ΔT_{\min}) is the minimum temperature difference between the hot stream and the cold stream in a heat exchanger. ΔT_{\min} is a constraint in the heat exchanger design that prevents a thermodynamic violation (for example temperature cross between the hot and cold stream). The heuristic put the limitation on ΔT_{\min} at 10 °C for shell and tube heat exchangers for effective heat transfer.³¹ Hence, the area of the heat exchanger in the simulations was selected to obtain a ΔT_{\min} greater than 10 °C.

Important results of the simulation are shown in Table 1. ΔT_{\min} in the heat exchanger at a pressure of 300 bar is higher than that at 250 bar. Since ΔT_{\min} of 10 °C is allowed, this implies a better heat integration potential for the process at 300 bar.

In addition, the extra heating (E-101 duty) required to raise the temperature of the preheated stream (#2) from the heat

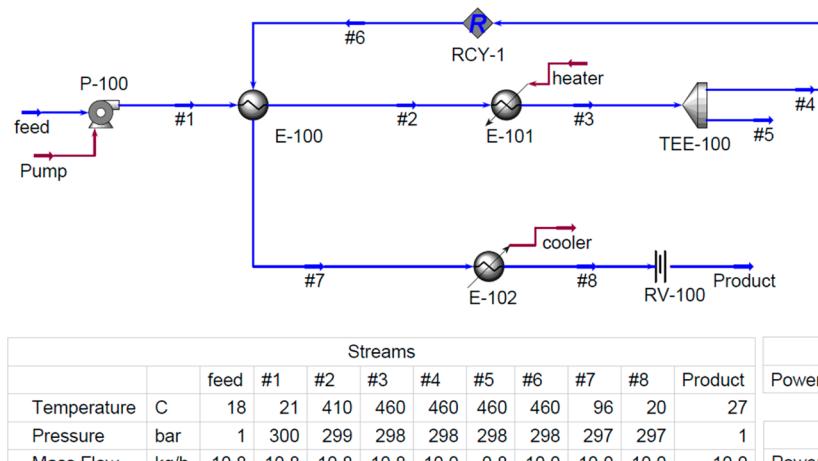


Figure 7. PFD of preliminary simulation based on water at 300 bar in UniSim Design.

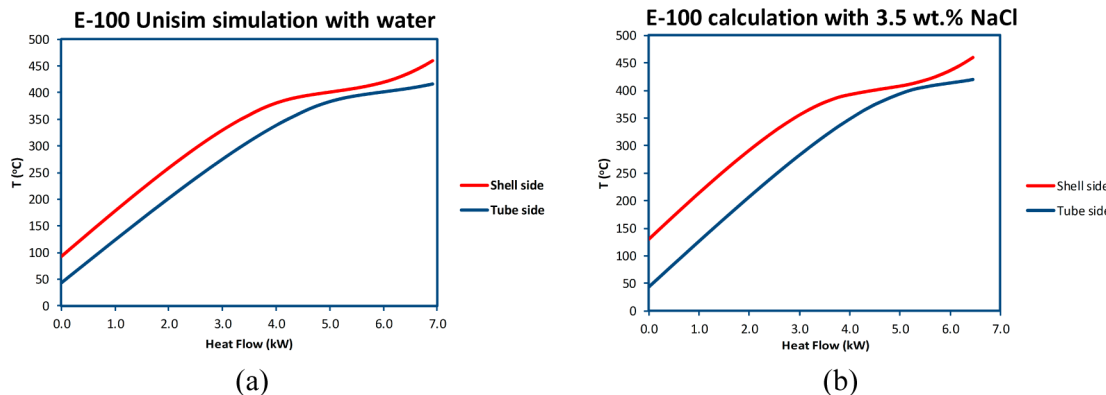


Figure 8. Temperature profile of heat exchanger E-100 from UniSim for water (a) and temperature profile calculated for 3.5 wt % NaCl (b) using the $P-T-X_{\text{NaCl}}-h$ correlation of Driesner.³²

exchanger to the desired operating temperature is lower (22% reduction) when the process is operated at 300 bar compared to operating at 250 bar. For system stability, heat integration potential and lower energy consumption, we have selected 300 bar as the operating pressure of the SCWD process.

A final process simulation of the SCWD process at 300 bar was then carried out utilizing the heat integration potential at 300 bar by increasing the heat exchange area from 0.15 to 0.21 m^2 ; this reduces the minimum approach temperature from 20 to 15 °C and the thermal energy consumption from 520 to 410 MJ_{th}/m³ product water (see Table 1, last column, 300^a).

The process design and simulation in UniSim was carried out using the properties of pure water neglecting the influence of the salt present on the process, especially the heat exchanger performance (complications such as possible temperature cross in the heat exchanger) and the energy required by the process. The effects of the presence of salt in solution on the system was checked by modeling the heat exchanger (E-100) using the $P-T-X_{\text{NaCl}}-h$ correlation developed by Driesner³² for a 3.5 wt % NaCl solution (feed concentration for the SCWD process) at 300 bar.

The temperature profiles in the heat exchanger (E-100) for the simulation in UniSim with water and for modeling a 3.5 wt % NaCl solution are shown in Figure 8 panels a and b, respectively. The profile for the two cases follow a similar trend, and there is no temperature cross in the heat exchanger for the 3.5 wt % case. A slight reduction in the heat exchanger duty (E-100 duty), the minimum approach temperature (E-100 ΔT_{\min}) was observed with the presence of salt (see Table 2). Also, a

In real seawater systems, there is potential for other salts such as CaSO_4 and MgSO_4 to precipitate on the walls of the heat exchanger because of their very low solubilities at the conditions in the heat exchanger (sub- to supercritical conditions). In the concentrated brine the solubility of these salts will be increased,³³ but whether this will be sufficient to avoid solid formation needs to be investigated. How the scaling can be handled will be the focus of subsequent research on the pilot plant.

5. DESIGN OF A PILOT UNIT

A proposed process design for the SCWD process for producing 10 kg/h of drinking water is shown in Figure 9 with the stream properties table added. The feed stream is pressurized and heated to a pressure of 300 bar and a final temperature of 460 °C in the separator. At these supercritical conditions, the stream is separated into a vapor (supercritical) phase and a liquid (concentrated brine) phase. The supercritical phase has a salt concentration of about 750 ppm, while the concentrated brine phase has a concentration of about 50 wt % NaCl. It is important not to go above 475 °C in order to prevent salt crystallization (see phase diagram, Figure 5) in the separator, which could lead to equipment blockage and by extension equipment failure.

Heat integration is very important in order to recover most of the energy put into the process and use that to reduce energy consumption. Therefore, the supercritical product stream is used to heat the cold feed stream in a counter-current heat exchanger. The feed stream goes through the tube, while the product stream passes through the shell. The extra heating required for the heated feed stream (#3) to be brought to the desired operating temperature is provided in the heated separator.

Kritzer²⁸ and Marrone and Hong³⁴ have identified the region just below the critical temperature as the maximum point of corrosion especially for chloride-containing streams; hence, the material of choice for this part of the process has to be one that is resistant to such a corrosive environment. The heat exchanger will be operating in such an environment, therefore, titanium grade 1 has been chosen as material of construction for the shell and tube.

The highly concentrated brine stream (#7) is moved into a crystallizer operated at much lower pressure (down to 1 bar) where the liquid is flashed to obtain salt and steam, which can be reused. The outlet of the heat exchanger shell is then cooled and depressurized to obtain drinking water of about 750 ppm

Table 2. Effect of the Presence of Salt on Simulation Results

$P = 300 \text{ bar}$	UniSim (H_2O)	3.5 wt % NaCl
E-100 duty (GJ/m ³ product water)	2.5	2.3
E-100 ΔT_{\min} (°C)	15	12
$A (\text{m}^2)$	0.21	0.21
E-101 duty (MJ/m ³ product water)	410	450

10% increase in the thermal energy required by the process (E-101 duty) was found for the 3.5 wt % NaCl case. Although the presence of 3.5 wt % NaCl in solution does have some slight effects on the heat exchange and energy requirement of the process, the simplification in the UniSim simulation with pure water is a good approximation for the real system. However, the thermal energy requirement obtained in the 3.5 wt % case will be taken as the thermal energy needed for the SCWD process.

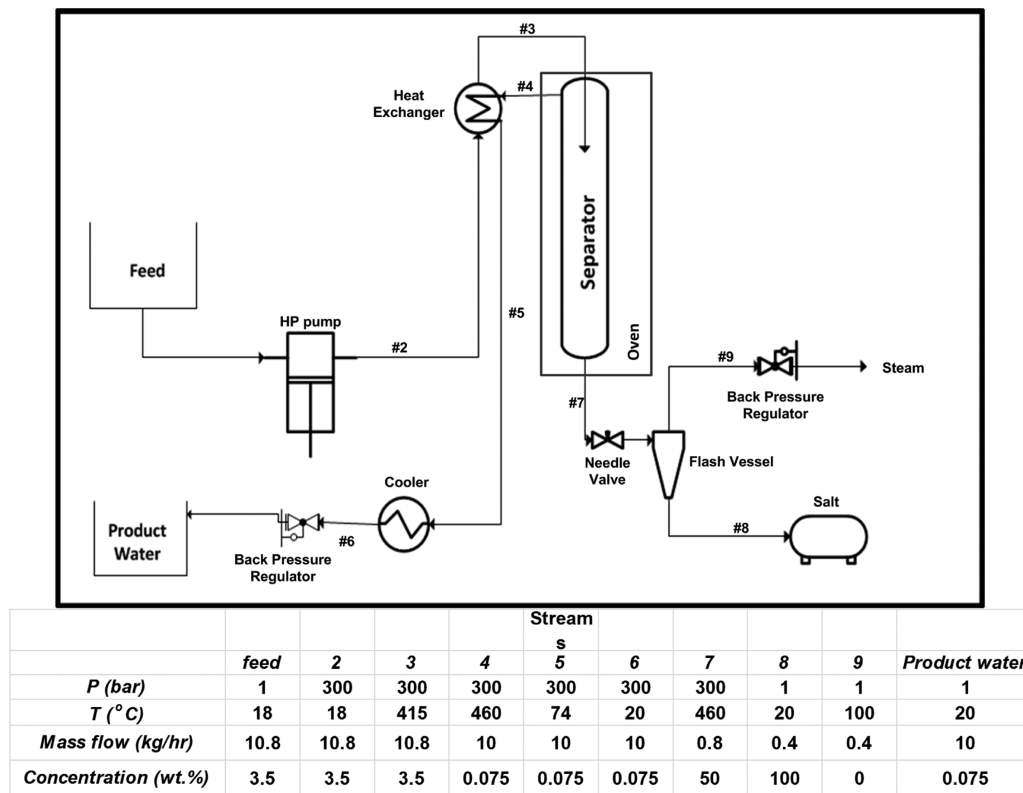


Figure 9. Proposed process design of a pilot unit for the SCWD process.

TDS (safe limit for drinking water is 1000 ppm³⁴). This pilot plant has been designed and is under construction. A subsequent paper (to be published) will report the results of measurements and performance of the pilot plant.

The estimated thermal energy consumption for this process is about 450 MJ_{th}/m³ drinking water, taking heat integration into account. The expected investment and operational costs direct the research to using the SCWD process as a post-treatment step for other conventional desalination methods.

6. CONCLUSIONS

A design of a pilot plant unit for the supercritical desalination of salt-water streams with zero liquid discharge has been presented. The phases present at supercritical conditions for a NaCl solution was studied in quartz capillaries. Under supercritical conditions, two distinct regions, V–L and V–S as well as a transition V–L–S were observed. The transition temperature from V–L to V–S was found to be about 450 °C at 250 bar, and 475 °C at 300 bar.

The phase equilibrium of NaCl–H₂O was studied under isobaric conditions in a lab-scale experimental setup. The solubility of NaCl in the vapor phase in the V–L region was found to decrease with increasing temperature and increase with increasing pressure. In addition, the phase equilibrium curve shifts upward and becomes narrower at the higher pressure of 300 bar. All results obtained are in agreement with literature (see Figure 5).

A lab-scale unit was designed, built, and operated at 300 bar and 460 °C to demonstrate the proof of principle of the SCWD process. A vapor phase (750 ppm of NaCl) and a concentrated liquid phase (50 wt % NaCl) were obtained under the process conditions. The 50 wt % brine was then flashed to atmospheric

pressure to produce fine salt crystals of 2–5 μm clustered together.

The SCWD process has been simulated in UniSim Design at 250 and 300 bar pressure with pure water only to mimic the process. Operating the SCWD process at 300 bar pressure was found to offer better heat integration potential as well as a 22% reduction in thermal energy consumption compared to 250 bar. As a result, 300 bar was selected as the operating pressure of the SCWD process.

A SCWD process with a two-stage (V–L at 300 bar, 460 °C and V–S at atmospheric pressure) separation step was designed for the production of 10 kg/h drinking water (*s* ≈ 750 ppm TDS) without the production of any waste stream (ZLD) as opposed to the conventional MSF and RO processes. The stand-alone thermal energy consumption is estimated at 450 MJ_{th}/m³.

■ AUTHOR INFORMATION

Corresponding Author

*E-mail: a.g.j.vanderham@utwente.nl.

Notes

The authors declare no competing financial interest.

■ ACKNOWLEDGMENTS

We gratefully acknowledge Wetsus, European Center of Excellence for Sustainable Water Technology (wetsus.nl), for its financial support for this project. The authors thank Magdalena Martinez Moral for her contribution to the experimental part (phase equilibrium) of this work.

■ NOTATIONS

A = area, m²

h = specific enthalpy, kJ/kg

i.d. = inside diameter, mm
 LMTD = logarithmic mean temperature difference, °C
 o.d. = outside diameter, mm
 P = pressure, bar
 ppm = parts per million
 SEM = scanning electron microscope
 T = temperature, °C
 TDS = total dissolved solids
 X_{NaCl} = mole fraction of sodium chloride
 U = overall heat transfer coefficient, W/m², °C
 V-L = vapor–liquid
 V-L-S = vapor–liquid–solid
 ZLD = zero liquid discharge

Greek Symbol

ΔT_{\min} = minimum temperature approach, °C

Subscripts

c = critical
 el = electrical
 min = minimum
 th = thermal

■ REFERENCES

- (1) Elimelech, M.; Phillip, W. A. The Future of Seawater Desalination: Energy, Technology, and Environment. *Science* **2011**, *333*, 712–717.
- (2) Cerci, Y.; Cengel, Y.; Wood, B.; Kahraman, N.; Karakas, E. S. *Improving the Thermodynamic and Economic Efficiencies of Desalination Plants: Minimum Work Required for Desalination and Case Studies of Four Working Plants*; University of Nevada: United States of America, 2003.
- (3) Miller, J. E. *Review of Water Resources and Desalination Technologies*; Sandia National Laboratories: New Mexico, 2003.
- (4) Wahlgren, R. V. Atmospheric Water Vapour Processor Designs for Potable Water Production: A Review. *Water Res.* **2001**, *35* (1), 1–22.
- (5) Wade, N. M. Distillation Plant Development and Cost Update. *Desalination* **2001**, *136*, 3–12.
- (6) Darwish, M. A.; Al-Najem, N. M. Energy Consumption by Multi-stage Flash and Reverse Osmosis Desalters. *Appl. Therm. Eng.* **2000**, *20*, 399–416.
- (7) Semiat, R. Desalination: Present and Future. *Water Int.* **2000**, *25* (1), 54–65.
- (8) Fritzmann, C.; Löwenberg, J.; Wintgens, T.; Melin, T. State-of-the-Art of Reverse Osmosis Desalination. *Desalination* **2007**, *216*, 1–76.
- (9) Lattemann, S.; Höpner, T. Environmental Impact and Impact Assessment of Seawater Desalination. *Desalination* **2008**, *220* (1 - 3), 1–5.
- (10) Nederlof, M. M.; van Paassen, J. A. M.; Jong, R. Nanofiltration Concentrate Disposal: Experiences in The Netherlands. *Desalination* **2005**, *178*, 303–312.
- (11) Anisimov, M. A.; Sengers, J. V.; Sengers, J. M. H. L., Near-Critical Behavior of Aqueous Systems. In *Aqueous Systems at Elevated Temperatures and Pressures: Physical Chemistry in Water, Steam and Hydrothermal Solutions*, 1st ed.; Palmer, D. A., Fernandez-Prini, R., Harvey, A. H., Eds.; Elsevier Ltd.: London, 2004; pp 29–71.
- (12) Marcus, Y. *Supercritical Water: A Green Solvent, Properties and Uses*; John Wiley & Sons: NJ, 2012.
- (13) Leusbroek, I.; Metz, S. J.; Rexwinkel, G.; Versteeg, G. F. Solubility of 1:1 Alkali Nitrates and Chlorides in Near-Critical and Supercritical Water. *J. Chem. Eng. Data* **2009**, *54*, 3215–3223.
- (14) Metz, S. J.; Leusbroek, I. Method and System for Supercritical Removal of an Inorganic Compound. WO2010011136A1, 2010.
- (15) Platen, B. C. v. Process for Removing Dissolved Salts from the Liquid Solvent. US2520186A, 1950.
- (16) Armellini, F. J.; Tester, J. W. Experimental Methods for Studying Salt Nucleation and Growth from Supercritical Water. *J. Supercrit. Fluids* **1991**, *4*, 254–264.
- (17) Armellini, F. J.; Tester, J. W.; Hong, G. T. Precipitation of Sodium Chloride and Sodium Sulfate in Water from Sub- to Supercritical Conditions: 150 to 550 °C, 100 to 300 bar. *J. Supercrit. Fluids* **1994**, *7*, 147–158.
- (18) Potic, B.; Kersten, S. R. A.; Prins, W.; van Swaaij, W. P. M. A High-Throughput Screening Technique for Conversion in Hot Compressed Water. *Ind. Eng. Chem. Res.* **2004**, *43* (16), 4580–4584.
- (19) Wagner, W.; Cooper, J. R.; Dittmann, A.; Kijima, J.; Kretzschmar, H. J.; Kruse, A.; Mareš, R.; Oguchi, K.; Sato, H.; Stöcker, I.; Šifner, O.; Takaishi, Y.; Tanishita, I.; Trübenbach, J.; Willkommen, T. The IAPWS Industrial Formulation 1997 for the Thermodynamic Properties of Water and Steam. *J. Eng. Gas Turbines Power* **2000**, *122* (1), 150–184.
- (20) Olander, A.; Liander, H. The Phase Diagram of Sodium Chloride and Water above the Critical Point. *Acta Chem. Scand.* **1950**, *4*, 1437–1445.
- (21) Parisod, C. J.; Plattner, E. Vapor–Liquid Equilibria of the NaCl–H₂O System in the Temperature Range 300–440 °C. *J. Chem. Eng. Data* **1981**, *26*, 16–20.
- (22) Bischoff, J. L.; Rosenbauer, R. J.; Pitzer, K. S. The System NaCl–H₂O: Relations of Vapor–Liquid near the Critical Temperature of Water and of Vapor–Liquid–Halite from 300 °C to 500°C. *Geochim. Cosmochim. Acta* **1986**, *50*, 1437–1444.
- (23) Sourirajan, S.; Kennedy, G. C. The System H₂O–NaCl at Elevated Temperatures and Pressures. *Am. J. Sci.* **1962**, *260*, 115–141.
- (24) Armellini, F. J.; Tester, J. W. Solubility of Sodium Chloride and Sulfate in Sub- and Supercritical Water Vapor from 450–550 °C and 100–250 bar. *Fluid Phase Equilib.* **1993**, *84*, 123–142.
- (25) Bischoff, J. L.; Pitzer, K. S. Liquid–Vapor Relations for The System NaCl–H₂O: Summary of The P–T–x Surface from 300° to 500 °C. *Am. J. Sci.* **1989**, *289*, 217–248.
- (26) Armellini, F. J. Phase Equilibria and Precipitation Phenomena of Sodium Chloride and Sodium Sulfate in Sub- and Supercritical Water. Ph.D. Thesis, Massachusetts Institute of Technology: MA, 1993.
- (27) Schubert, M.; Regler, J. W.; Vogel, F. Continuous Salt Precipitation and Separation from Supercritical Water. Part 1: Type 1 Salts. *J. Supercrit. Fluids* **2010**, *52*, 99–112.
- (28) Kritzer, P. Corrosion in High-Temperature and Supercritical Water and Aqueous Solutions: A Review. *J. Supercrit. Fluids* **2004**, *29*, 1–29.
- (29) UNESCO–WWAP *Water for People, Water for Life*; UNESCO: 2003.
- (30) Linke, W. F. *Solubilities—Inorganic and Metal Organic Compounds*; American Chemical Society: Washington, DC, 1958.
- (31) Heggs, P. J. Minimum Temperature Difference Approach Concept in Heat Exchanger Networks. *Heat Recovery Syst. CHP* **1989**, *9* (4), 367–375.
- (32) Driesner, T. The System H₂O–NaCl. Part II: Correlations for Molar Volume, Enthalpy, and Isobaric Heat Capacity from 0 to 1000 °C, 1 to 5000 bar, and 0 to 1 X_{NaCl} . *Geochim. Cosmochim. Acta* **2007**, *71*, 4902–4919.
- (33) Blouinot, C. W.; Dickson, F. W. The Solubility of Anhydrite (CaSO₄) in NaCl–H₂O from 100 to 450 °C and 1 to 1000 bar. *Geochim. Cosmochim. Acta* **1969**, *33* (2), 227–245.
- (34) Marrone, P. A.; Hong, G. T. Corrosion Control Methods in Supercritical Water Oxidation and Gasification Processes. *J. Supercrit. Fluids* **2009**, *51*, 83–103.